2019

Detection of Sickle Cell Disease-associated Single Nucleotide Polymorphism Using a Graphene Field Effect Transistor

Kandace Fung
Claremont McKenna College

Detection of Sickle Cell Disease-associated Single Nucleotide Polymorphism Using a Graphene Field Effect Transistor

A Thesis Presented

by

Kandace Fung

To the Keck Science Department

Of Claremont McKenna, Pitzer, and Scripps Colleges

In partial fulfillment of

The degree of Bachelor of Arts

Senior Thesis in Biology

April 29th, 2019

Table of Contents

Abstract

Sickle Cell Disease (SCD) is a hereditary monogenic disorder that affects millions of people worldwide and is associated with symptoms such as stroke, lethargy, chronic anemia, and increased mortality. SCD can be quickly detected and diagnosed using a simple blood test as an infant, but as of now, there is currently limited treatment to cure an individual of sickle cell disease. Recently, there have been several promising developments in CRISPR-Cas-associated gene-editing therapeutics; however, there have been limitations in gene-editing efficiency monitoring, which if improved, could be beneficial to advancing CRISPR-based therapy, especially in SCD. The CRISPR-Chip, a three-terminal graphene-based field effect transistor (gFET), was used to detect genomic samples of individuals with SCD, with and without amplification. With the dRNP-HTY3' complex, CRISPR-Chip was able to specifically detect its target sequence with and without pre-amplification. With the dRNP-MUT3' complex, CRISPR-Chip was only able to specifically detect one of its two target sequences. Facile detection, analysis, and editing of sickle cell disease using CRISPR-based editing and monitoring would be beneficial for simple diagnostic and gene-editing therapeutic treatment of other single nucleotide polymorphisms as well, such as beta-thalassemia and cystic fibrosis.

Introduction

Sickle Cell Disease (SCD) is a hereditary monogenic disorder that affects millions of people worldwide and is associated with symptoms such as stroke, lethargy, chronic anemia, and increased mortality (Bialk et al., 2016; Park et al., 2016). SCD includes all genotypes with at least one sickle gene and is caused by a single nucleotide polymorphism (SNP) in the β-globin gene (HBB) on chromosome 11, converting a GAG codon to a GTG codon in exon 1 (Bialk et al., 2016; Park et al., 2016). SCD can be quickly detected and diagnosed using a simple blood test as an infant; however, there is currently limited treatment to cure an individual of sickle cell disease. As of now, allogeneic hematopoietic stem cell transplantation (HSCT) is the only treatment available. HSCT for SCD uses donor allogeneic stem cells from a family-related or an unrelated donor, from the bone marrow, peripheral blood or cord blood (Galgano and Hutt, 2018). These stem cells are then intravenously infused into patients with SCD. This treatment is an invasive procedure associated with high risk of graft-versus-host-disease, infections, and infertility, and is only feasible for approximately 15% of the patient population due to lack of compatible human leukocyte antigen (HLA)-matched donors (Kassim and Sharma, 2017; Park et al., 2016).

In recent years, researchers have utilized multiple techniques to improve upon HSCT therapies in order to cure SCD. These techniques include viral vector-based donor templates and gene-editing methods such as zinc finger nucleases (ZFNs), transcription activator-like effector nucleases (TALENs), and clustered regularly-interspaced Short palindromic repeats (CRISPR)-associated nuclease (Cas) (Demirci et al., 2018; Gupta

and Musunuru, 2014; Lux et al., 2019; Moran et al., 2018; Sebastiano et al., 2011; Sun and Zhao, 2014; Tasan et al., 2016).

CRISPR-Cas9-based gene-editing technology

Compared to the other methods, CRISPR-Cas is inexpensive and demonstrates higher ease of use and modifiability (Gupta and Musunuru, 2014; Tasan et al., 2016). CRISPR-Cas9 uses a 20-nucleotide single-stranded guide RNA (sgRNA) sequence that is complementary that is adjacent to a protospacer adjacent motif (PAM), usually NGG (Anders et al., 2014; Aryal et al., 2018). CRISPR-Cas9's modifiability comes from only needing to change the 20-nucleotide sgRNA sequence to target any genomic sequence (Gupta and Musunuru, 2014). However, Cas9 protein size and CRISPR-Cas9's off-target effects are the two main concerns regarding the CRISPR-Cas9 gene-editing method. Compared to the other two popular gene-editing methods, ZFN and TALENS, CRISPR-Cas9 is significantly larger in size, making it more difficult to deliver using viral vectors or as an RNA molecule (Gupta and Musunuru, 2014).

While CRISPR-Cas9's specificity and binding are attributed to its 20 nucleotide protospacer and the PAM, there have been reports of off-target cleavage activity and varying levels of on-target efficiency depending on the sgRNA sequence selected (Aryal et al., 2018; Fu et al., 2013; Hsu et al., 2013; Pattanayak et al., 2013). However, since these off-target effects usually stem from the sgRNA sequence, this issue can be mitigated by choosing a sgRNA sequence with the least known off-target effects. It is also important to note that many reports of high-frequency off-target activity have been associated with human and mouse cell-lines, but there have been few reports of off-target

effects in mammalian embryo editing (Hsu et al., 2013; Iyer et al., 2018; Nakajima et al., 2016). One study done demonstrated CRISPR-Cas9's efficiency of 80% in targeting both alleles of two genes in mice, which indicates CRISPR-Cas9 as a promising tool in gene-editing therapeutics (Wang et al., 2013).

Multiple studies have used CRISPR/Cas9 genome editing technology to correct the sickle cell mutation in CD34+ hematopoietic stem and progenitor cells (HSPCs) and have demonstrated relatively high editing efficiencies and clinically relevant gene-editing rates (DeWitt et al., 2016; Hoban et al., 2016; Lin et al., 2017; Park et al., 2016; Tasan et al., 2016). These results are indicative of the possible applications of CRISPR/Cas9 in targeting the specific mutation in SCD. Using CD34+ HSPCs from patient with SCD, one lab used CRISPR-Cas9 with a single-stranded DNA oligonucleotide donor (ssODN) to achieve efficient correction of the SCD mutation in human HSPCs (DeWitt et al., 2016). The edited HSPCs produced less sickle hemoglobin RNA and protein, as well as demonstrated increased levels of wild-type hemoglobin upon differentiating into erythroblasts. Immunocompromised mice were treated *ex vivo* with engraftment of the human HSPCs, and the HSPCs maintained the SCD gene edits for sixteen weeks at levels indicative of having clinical benefit.

Another study used both TALENs and CRISPR-Cas9 methods to target the sickle cell mutation in HBB to evaluate on-target and off-target cleavage rates (Hoban et al., 2016). To measure these gene modification rates through homology directed repair (HDR), they co-delivered TALENs and CRISPR-Cas9 to K562 3.21 cells, which contain the sickle mutation, with a homologous donor template containing the HBB gene. While

TALENs demonstrated average gene modification rates between 8.2% - 26.6%, CRISPR-Cas9 produced an overall higher rate of 4.2 - 64.3% and thus was chosen to facilitate SCD correction in HSPCs. CRISPR-Cas9 delivery to HSPCs demonstrated *in vitro* gene modification rates in HSPCs at over 18%. To test CRISPR-Cas9's clinical applications, the lab corrected the SCD mutation in bone-marrow derived CD34+ HSPCs from patients with SCD, which resulted in wild-type hemoglobin production, further supporting CRISPR-Cas9's use as gene-editing tool for patient with SCD. Current methods of *ex vivo* CRISPR/Cas9-based gene-editing techniques have only been tested *in vitro* human cell cultures or *in vivo* mouse models, and there are currently no research trials involving humans directly (DeWitt et al., 2016; Hoban et al., 2016). However, clinical trials are on the horizon, meaning CRISPR-Cas9 *ex vivo* editing of SCD-associated mutations will need to be constantly monitored before any potential reintroduction into patients.

Besides genome editing, gene therapy monitoring and diagnostics are emerging applications in the CRISPR-Cas systems (Mintz et al., 2018; Uppada et al., 2018). In a recent study, researchers developed a new technology with sensitivity and specificity in detecting unamplified target DNA sequences with the insertion of the *bfp* (blue fluorescent protein) gene and large fragment deletions relevant in Duchenne muscular dystrophy clinical samples (Hajian et al., 2019). This new technology termed CRISPR-Chip, a graphene-based field effect transistor with CRISPR/dCas9 immobilized on the surface, has potential to play a part in the development of CRISPR-based therapy as a gene-editing monitoring tool.

Conventional nucleic acid-based detection methods require amplification of the target genome sequences, such as PCR, in order to validate the presence of a target gene (Cao et al., 2017; Hudecova, 2015). In addition, many nucleic acid detection technologies are expensive, require multi-step processes as well as bulky, complex instruments, which are time-consuming and require trained personnel for operation. CRISPR-Chip overcomes these limitations as it is a hand-held, label-free device that is affordable, easy to use, and only requires a short amount of time for target gene detection.

CRISPR-Chip background information

CRISPR-Chip is comprised of two main parts: its graphene-based field effect transistor (gFET) platform and an immobilized CRISPR-nuclease dead cas9 (dcas9) protein complex. This graphene substrate was chosen as it is known for its excellent electrical conductivity, large surface area, and high sensitivity to the adsorption and interactions of charged molecules (Peña-Bahamonde et al., 2018; Pumera, 2011). The CRISPR-Chip is a CRISPR-enhanced, three-terminal gFET, with source, drain, and liquid-gate electrodes as shown in Figure 1 (Hajian et al., 2019).

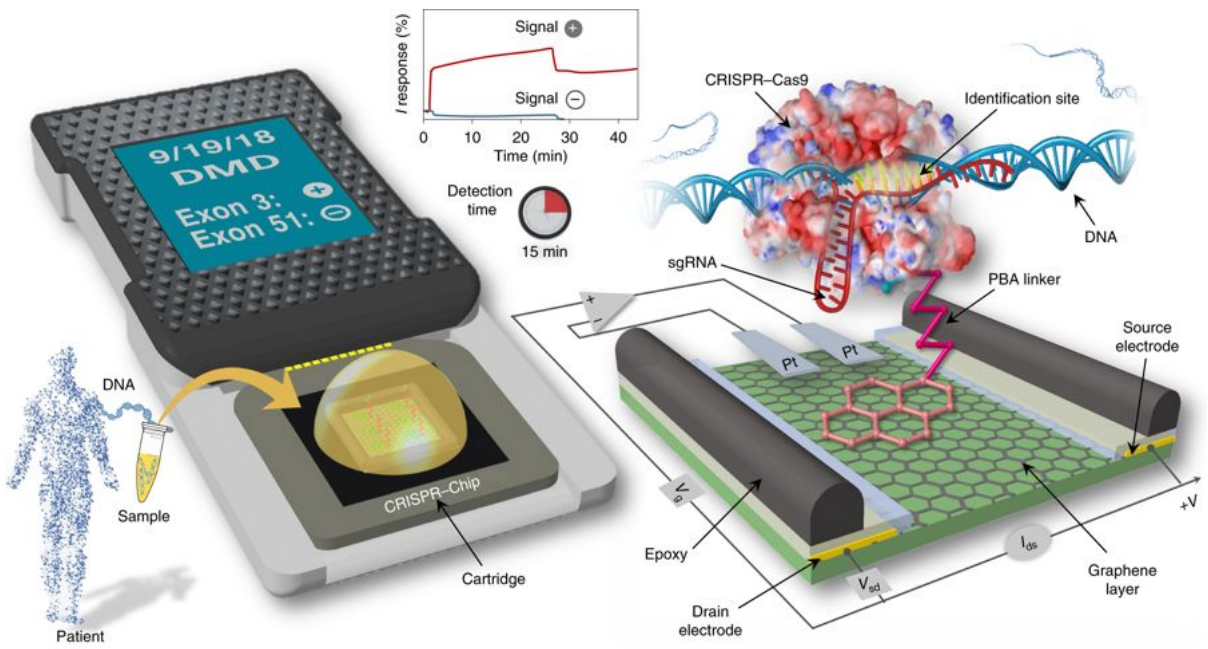

Figure 1. CRISPR-Chip graphic: the CRISPR-Chip, a graphene field effect transistor, with immobilized dCas9 and sgRNA is able to detect its target sequence. Reproduced from "Detection of unamplified target genes via CRISPR–Cas9 immobilized on a graphene field-effect transistor," by R. Hajian et al., 2019, *Nature Biomedical Engineering*. Copyright 2019 by Springer Nature. Reprinted with permission.

The immobilized dead cas9 protein complex contains a 20-nucleotide single-stranded guide-RNA (sgRNA) molecule bound as a ligand. This complex is termed as dRNPs (dead cas9- ribonucleoproteins) hereafter. The sgRNA can be easily designed to complement a specific target sequence. The designs of the sgRNAs used in this study will be discussed in the Materials and Methods section (pg. 14). The dRNP, similar to CRISPR-Cas9 activity, will probe the entire genomic sample until it finds its target sequence; however, since the NUC lobe of the dcas9 is catalytically inactive,

instead of cleaving its target sequence, the dRNP will unzip the double helix and the sgRNA will bind upstream of the protospacer adjacent motif (PAM) (Boyle et al., 2017; Jiang and Doudna, 2017).

The biosensor is functionalized with dRNP immobilization onto the graphene chip via a molecular linker, 1-pyrenebutanoic acid (PBA). First, PBA non-covalently binds with the graphene surface through π–π aromatic stacking interactions, followed by covalent binding of PBA's carboxylate group to the dCas9 protein, tethering the protein onto the CRISPR-Chip. As shown in Fig 2, any PBA molecules that do not have any attached dCas9 will be blocked by amino-polyethylene glycol 5-alcohol (PEG); however, what is not shown in the figure, subsequent addition of ethanolamine hydrochloride. These blocking molecules (known in the protocol as Quench 1 and Quench 2) are important as they hinder any non-specific adsorption or binding of charged molecules onto the graphene surface. After immobilizing dCas9 onto and saturating the graphene platform, sgRNA is added onto the chip to conjugate with the dCas9 to create the dRNP complex. More information on the protocol can be found in the Materials and Methods section (pg. 17-19).

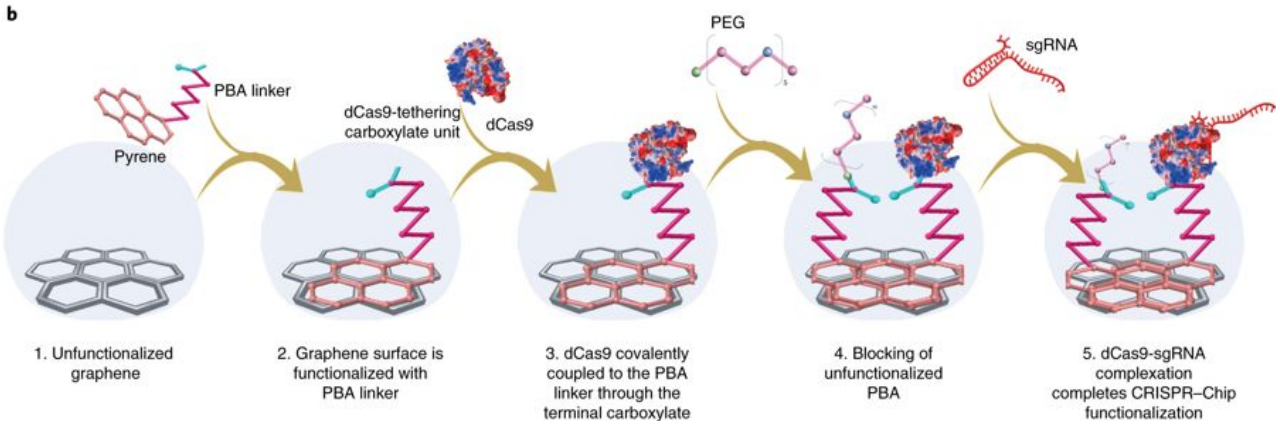

Figure 2. Schematic of CRISPR-Chip functionalization. Adapted from "Detection of unamplified target genes via CRISPR–Cas9 immobilized on a graphene field-effect transistor," by R. Hajian et al., 2019, *Nature Biomedical Engineering*. Copyright 2019 by Springer Nature. Reprinted with permission.

The CRISPR-Chip is inserted to a hand-held reader that is connected to a computer program which displays the response. The functionalization of the graphene surface acts as a channel between the source and drain electrodes, with the third terminal being a liquid gate that interacts with the genomic sample which is contained in a reaction buffer. Voltage is applied across the surface between the liquid-gate and source electrodes (Vg). Due to graphene's sensitivity to interactions with charged molecules on its surface, binding of the negatively-charged target DNA to the RNP will modify the conductivity of graphene, and this binding will be read by the CRISPR-Chip reader as an electrical current. Binding of the target DNA with the dRNP will result in a larger electrical output signal from the reader while minimal binding of non-target DNA with the dRNP will result in a significantly smaller electrical response. For more detailed

description of the CRISPR-Chip operational and measurement methods, please refer to the Hajian 2019 paper.

Earlier this year, the CRISPR-Chip successfully analyzed DNA samples collected from HEK293T cell lines that expressed *bfp* and clinical samples of DNA of patients with Duchenne muscular dystrophy (DMD) (Hajian et al., 2019). They were able to detect and differentiate genomic samples of DNA with and without *bfp* or DMD. The lab tested two different clinical samples of DMD: one containing deletion of exon 3 and the other containing deletion of exon 51. They used clinical samples of healthy patients as a control. The CRISPR-Chip detection of DMD is a break-through technology as it can be used as an inexpensive and facile diagnostic tool in a clinical setting. In addition, the ability of the CRISPR-Chip to detect target sequences in a genomic sample without amplification of the target sequence demonstrates its sensitivity and specificity.

Single nucleotide polymorphisms

A single nucleotide polymorphism (SNP) is a single nucleotide base mutation, in which one of the bases (A, T, C, G) are replaced with another base. Sickle cell disease is caused by a SNP, and while it is one of the diseases that can be easily diagnosed by a simple blood test, detecting SNPs in general has proven difficult. Current methods of detecting SNPs require complex processes and amplification of the target sequence in order to achieve detection and have poor specificity and sensitivity (Ficht et al., 2004; Gerion et al., 2003; Xiao et al., 2009). Recently, there has been more development in

using electrical biosensors, which have lowered the limit of detection of target DNA to the femtomolar level (Lu et al., 2014; Ping et al., 2016).

Objective

In this study, I hypothesize that we will be be able to use the CRISPR-Chip platform to detect the sickle cell disease-associated SNP without amplification. Compared to the indels from the *bfp* gene and from the mutations in DMD, the sickle cell associated-SNP may be more difficult to detect from unamplified genomic samples as the SCD target sequence only has one base pair difference to a healthy genomic sequence, as well as due to the promiscuity of the CRISPR-Cas system (Tsai et al., 2017). If a sgRNA has high off-target activity, this may inhibit our ability to detect a single mismatch in the dRNP target sequence. As the CRISPR-Cas9 gene-editing technology is already known for its off-target effects, this may be a challenge for using the CRISPR-Chip to detect a SNP. However, successes of SCD correction in HSPCs using CRISPR-Cas9 shown in previous literature, as well as the sensitivity and specificity of the CRISPR-Chip, are promising in optimizing the CRISPR-chip device in detecting the SCD-associated SNP (DeWitt et al., 2016; Hajian et al., 2019; Hoban et al., 2016).

Materials and Methods

Single guide RNA (sgRNA) design

For sickle cell disease (SCD) analysis via CRISPR-Chip, 3 sgRNAs were designed utilizing multiple sgRNA designing programs and a sgRNA used in previous literature (Bialk et al., 2016). The HBB gene was input into these programs, and the sgRNA sequences chosen targeted sequences in exon 1 where the single point mutation causing SCD was located. The first sgRNA sequence, termed sgRNA MUT 3', targeted a sequence with the SCD mutation: 5' GTAACGGCAGACTTCTCCAC 3'. The sgRNA was named sgRNA MUT3' because the SCD mutation is the second base pair from the 3' end. sgRNA MUT3' was designed based off of online sgRNA design programs: GUIDES Designer, Chop Chop, CRISPOR, and Synthego. The second sgRNA sequence, termed sgRNA MUT 5', targeted a different sequence with the same SCD mutation: 5' CTCAGGAGTCAGATGCACCA 3'. sgRNA MUT5' was termed this name because the SCD mutation is the second base pair from the 5' end. sgRNA MUT5' was designed based off of online sgRNA design programs: DNA 2.0, CRISPOR, and Synthego. The third sgRNA sequence, termed sgRNA HTY 3', targeted the same sequence as sgRNA MUT3' without the SCD mutation: 5' GTAACGGCAGACTTCTCCTC 3'. sgRNA HTY3' was generated by online sgRNA design programs: GUIDES Designer, Chop Chop, CRISPOR, and Synthego. In addition, sgRNA HTY3' has also been successfully used to cleave the target sequence in previous literature (Bialk et al., 2016).

sgRNA selection and design schematic

Target sequence: 5’ GTAACGGCAGACTTCTCC**T**C 3’

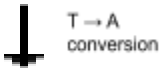

Sickle cell mutation: 5’ GTAACGGCAGACTTCTCC**A**C 3’

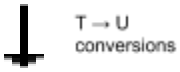

sgRNA sequence: 5’ GUAACGGCAGACUUCUCC**A**C 3’

sgRNA sequences (5’ to 3’)

sgRNA MUT 3’: GUAACGGCAGACUUCUCC**A**C

sgRNA HTY 3’: GUAACGGCAGACUUCUCC**U**C

sgRNA MUT 5’: C**A**CAGGAGUCAGAUGCACCA

Primer selection

For validation of the designed sgRNAs, primers were designed using Thermo Fisher Scientific’s Primer Design Tool. The HBB gene was inputted into the program, and 3 paired primers that encompassed the entirety of exon 1 were produced. All 3 paired primers were guaranteed to have a 95% success rate in sequencing viability, and the longest amplicon length (506 base pairs) was chosen as caution to capture the entire exon 1 and for better visibility during PCR. The forward and reverse primer sequences were TTGAGGTTGTCCAGGTGAGCCA and GGCCAATCTACTCCCAGGAGCA respectively.

Genomic DNA sample selection

Human genomic samples from two male patients affected by sickle cell disease were purchased with certificate of analysis from Coriell Institute for Medical Research (Camden, NJ). Sample SCD1 (NA16265) is a sample from a 19-year old African American male with homozygous sickle cell diseases (HbSS). Sample SCD2 (NA16267) is a sample from a 3-year old African American male with two copies of the sickle cell mutation. The concentrations were routinely measured prior to incubation with CRISPR-Chip using Infinite M200 Nanoquant (Tecan).

PCR protocol

HBB exon 1 was amplified from 100ng *genomic* DNA via PCR according to manufacturer's protocols. In a 50µL reaction mixture, the following reagents were used: 100ng genomic DNA (NA16265, NA16267), 10 µL 5X Phusion HF Buffer, 1 µL dNTP, 5 µL forward primer, 5 µL reverse primer, 0.5 µL Phusion DNA polymerase and, X µL H2O (X denotes the remaining solution needed to create a 50µL mixture). The following PCR thermal cycler protocol was used (PTC-100: Programmable Thermal Controller, MJ Research Inc., U.S.): (1) 98˚C for 30 sec (2) 98˚C for 10 sec (3) 63.5˚C for 30 sec (4) 72˚C for 15 sec (5) repeat 2-4 29x (6) holding at 72˚C for 5 min prior to cooling to 4˚C. The forward and reverse primer sequences were TTGAGGTTGTCCAGGTGAGCCA and GGCCAATCTACTCCCAGGAGCA respectively. 2 µL of the PCR products were loaded on a 1% agarose gel 100V for 1hr, followed by an ethidium bromide bath

(0.5µg/ml, 30min). Once stained, the gel was imaged using the UVP ChemStudio (Analytikjena, Germany)

CRISPR-Chip Molecular Linker Functionalization and Activation

Naked graphene FET chips were obtained (Cardea, San Diego CA) and cleaned with 30µL acetone twice and 30µL deionized water (DIW) once. The chips were subsequently functionalized with 1-pyrenebutanoic acid (PBA) (5mM, 15 µl) in dimethylformamide (DMF) for 2 hours at room temperature or overnight at 4˚C. Following the incubation, the graphene sensor was rinsed with 30µL DMF twice and 30µL DIW once. The PBA was activated using a 1:1 volume ratio of N-(3-Dimethylaminopropyl)-N′-ethylcarbodiimide hydrochloride (EDC, 4mM) and N-hydroxysuccinimide (NHS, 11mM) (Sigma Aldrich) in 50 mM of 2-(N-Morpholino) ethanesulfonic acid (MES, pH 6) for 5 minutes at room temperature according to published literatures prior to incubation with dCas9 (Everaerts et al., 2008; Wang et al., 2011).

CRISPR–Chip evaluation for the detection of SCD in the presence of Amplicons

The dRNP-HTY3’ and dRNP-MUT3’ functionalized CRISPR-Chips were calibrated with 2mM MgCl2 for 5min at 37 °C and subsequently incubated with 900ng of amplicons SCD1 or SCD2 (30 µl in 2mM MgCl2) for 25min at 37 °C. For the control experiments, amplicons of healthy DNA without the SCD mutation or amplicons without

the HBB sequence were incubated with dRNP-HTY3'- and dRNP-MUT3'-functionalized CRISPR–Chips. For all experiments, the sensor was rinsed (2mM MgCl2, 30 µl) for 15min at 37 °C after incubation with the genomic sample.

CRISPR–Chip detection of SCD in the presence of Genomic DNA

The dRNP-HTY3'-functionalized CRISPR–Chips were calibrated with 2mM MgCl2 for 5min at 37 °C and subsequently incubated with 1800ng SCD1 or SCD2 DNA (30µl in 2mM MgCl2). For the control experiments, 1800ng of healthy human embryonic kidney (HEK) DNA was incubated with dRNP-HTY3'-functionalized CRISPR-Chips. For all experiments, the CRISPR–Chip response was continuously monitored for 25 minutes at 37 °C. CRISPR–Chips were then rinsed (2mM MgCl2, 30 µl) for 15 minutes at 37 °C after incubation with the genomic sample. 1800ng genomic DNA was used instead of 900ng because initial tests of 900ng genomic DNA samples were too low.

CRISPR-Chip Complete Assay Protocol

1. Calibration of PBA-functionalized chips with 50mM MES for 5 minutes.
2. Activate the PBA linker with a mixture of 4mM EDC and 11mM NHS for 5 minutes.
3. Rinse any unbound PBA linker with 50mM MES (2x) for 1 minute.
4. Association of the PBA linker with 900ng (30 µl in 2 mM MgCl2) dCas9 for 15 minutes.
5. Association of Quench 1 containing 1mM amino-PEG5-alcohol for 10 minutes.

6. Association of Quench 2 containing 1M ethanolamine hydrochloride for 10 minutes.
7. Rinse any unbound Quench 1 and Quench 2 with 2mM $MgCl_2$ (5x) for 1 minute.
8. Calibration for sgRNA with 2mM $MgCl_2$ for 5 minutes.
9. Association of 900ng (30 µl in 2 mM MgCl2) sgRNA for 10 minutes.
10. Rinse away any unbound sgRNA and calibrate for DNA with 2mM $MgCl_2$ for 5 minutes.
11. Association of Xng (30 µl in 2 mM MgCl2) DNA for 25 minutes. (X= 900ng or 1800ng, depending on the type of sample used).
12. Rinse of any unbound DNA with 2mM $MgCl_2$ for 15 minutes.

CRISPR-Chip Sensor Response, Measurement, and Analysis Methods

The sensor response was recorded in real-time as shown in Figure 3, and the data were analyzed using equation below, which was used in previous literature (Hajian et al., 2019). Each chip consists of three transistors that separately measure the current, and these individual transistor responses can be analyzed separately. I_{ds} is the signal after incubation with the DNA sample and subsequent rinsing. I_{ds0} is the calibration baseline signal after the assay buffer was incubated during calibration. The calibration step takes into account sensor-to-sensor variation and effects of the buffer. I-response (%) the unit of measure, is the percentage change in between I_{ds0} (calibration baseline) and I_{ds} (the response after rinsing of the target DNA).

$$\text{I-response (\%)} = \frac{100(Ids - Ids0)}{Ids0}$$

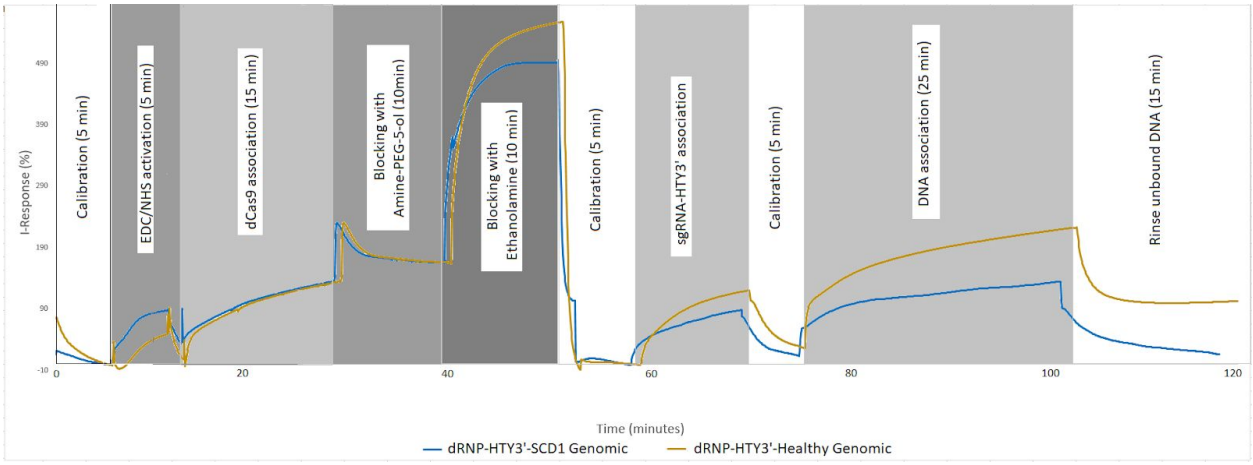

Figure 3. Real-time CRISPR-Chip I-Response (%), average current, is monitored throughout sensor functionalization and analysis with dRNP-HTY3'. The yellow line indicates the I-Response (%) of dRNP-HTY3'-Healthy Genomic DNA and the blue line indicates the I-Response (%) of dRNP-HTY3'-SCD1 Genomic DNA. The white regions represent rinsing and calibration with 2mM MgCl2.

Results

Selectivity of the immobilized dRNP-HTY3' with amplicon sequences

CRISPR-Chip's detection of the SCD mutation was first tested using amplicon sequences of two different DNA samples containing the SCD mutation. The first control was amplicon sequences from healthy DNA without the SCD mutation, and the second control (Scram) was amplicon sequences that did not include the HBB gene sequence. The PCR protocol for DNA amplification can be found in the Methods section. Each combination of dRNP-HTY3' with (900ng Amplicon) was ran at least three times.

I found evidence to support selective binding and detection of dRNP-HTY3' for Healthy amplicon. The average responses of the four amplicon samples (Healthy, SCD1, SCD2, and Scram) were different, with Healthy amplicon with the highest average response at 10.04 and Scram amplicon with the lowest response at 5.67 (One-Way ANOVA: $F_{3, 39} = 8.044$, $p = 0.000272$, Fig. 4). A post-Tukey test was performed and further supports dRNP-HTY3' complex's higher affinity of binding with Healthy amplicon. The results are shown in the Table 1 (* notes statistical significance).

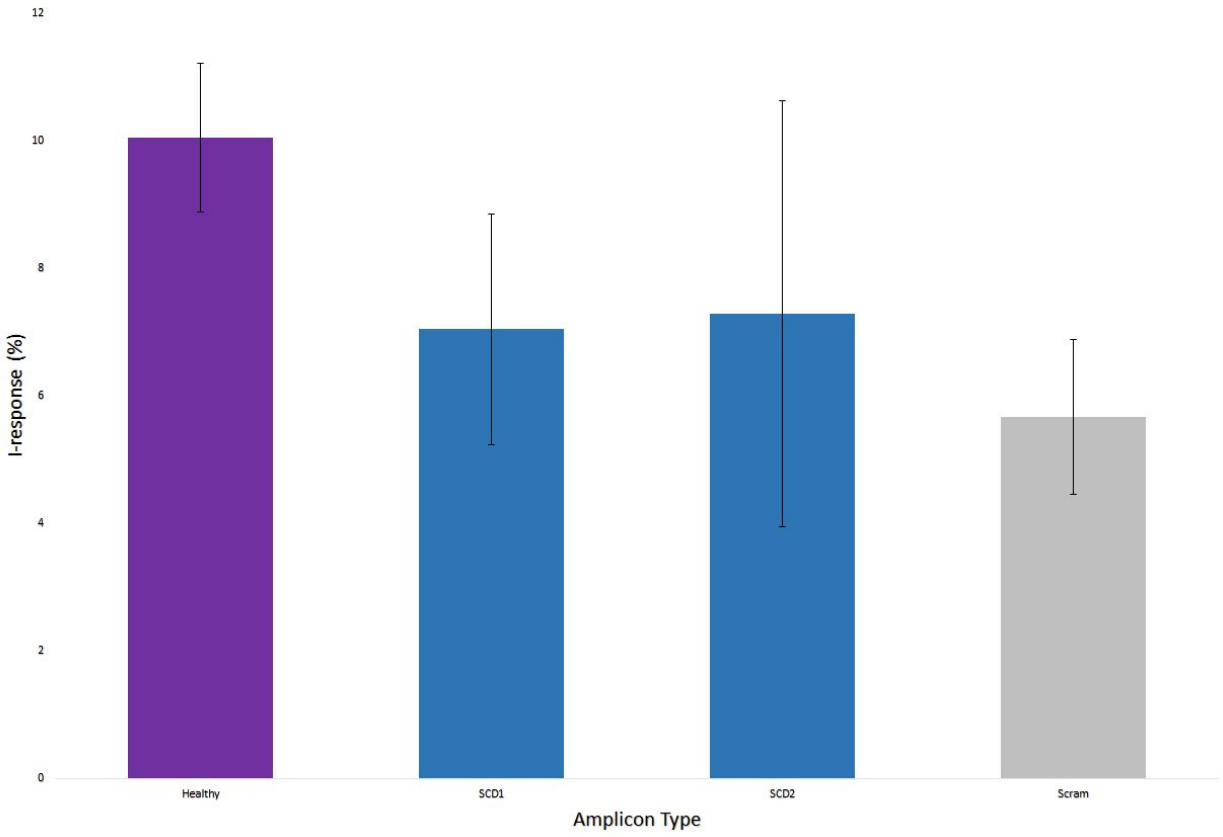

Figure 4. The relationship between dRNP-HTY3' (900ng amplicon type) and average I-Response (%). Bar heights and bars represent means ± standard deviation. Healthy (n=10), SCD1 (n=15), SCD2 (n=9), Scram (n=9) (n= number of working transistors).

Table 1. Post-Tukey analysis of dRNP-HTY3' sensor responses of amplicon samples

Amplicon Comparison	P-adjusted value
Healthy-SCD1 *	0.0042601
Healthy-SCD2 *	0.0251331
Healthy-Scram *	0.0001736
SCD1-SCD2	0.9917302
SCD1-Scram	0.3807639
SCD2-Scram	0.3361175

Specificity of the immobilized dRNP-HTY3' with genomic sequences

Genomic DNA samples of Healthy DNA extracted from HEK cells and the two different DNA samples containing the SCD mutation were tested with the dRNP-HTY3' complex. Each combination of dRNP-HTY3' with (1800ng Genomic Sample) was ran at least two times.

I found evidence to support selective binding and detection of dRNP-HTY3' for Healthy amplicon. The average responses of the three genomic samples (Healthy, SCD1, and SCD2) were different, with Healthy genomic sample with the highest average response at 4.48 and SCD1 genomic sample with the lowest response at 0.57 (One-Way

ANOVA: $F_{2, 24} = 58.87$, p = 5.55e-10, Fig. 5). A post-Tukey test was performed and further supports dRNP-HTY3' complex's higher affinity of binding with Healthy genomic sample. The results are shown in the Table 2 (* notes statistical significance).

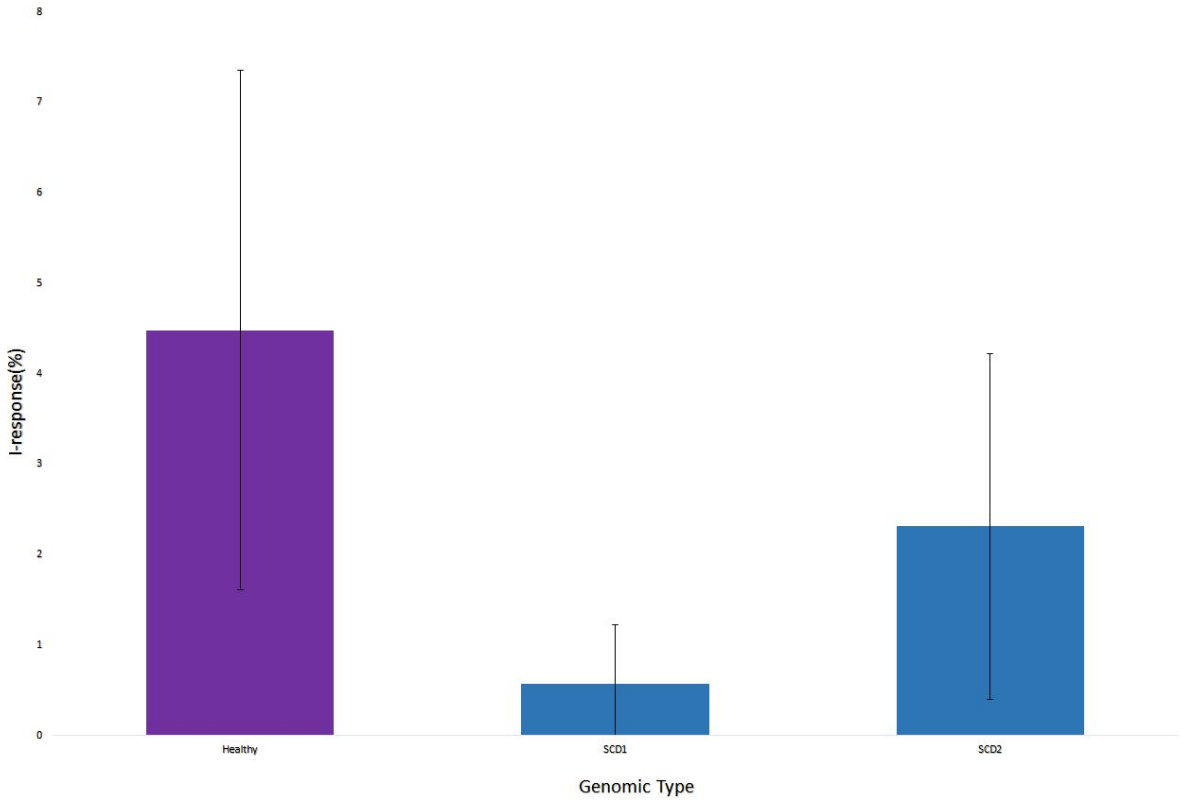

Figure 5. The relationship between dRNP-HTY3' (1800ng genomic type) and average I-Response (%). Bar heights and bars represent means ± standard deviation. Healthy (n=6), SCD1 (n=12), SCD2 (n=9) (n= number of working transistors).

Table 2. Post-Tukey analysis of dRNP-HTY3' sensor responses of genomic samples

Amplicon Comparison	P-adjusted value
Healthy-SCD1 *	0.0000000
Healthy-SCD2 *	0.0000003
SCD1-SCD2 *	0.0082045

Specificity of the immobilized dRNP-MUT3' with amplicon sequences

We tested for selectivity of the SCD SNP using the dRNP-MUT3' complex with the four amplicons tested previously with dRNP-HTY3'. Each combination of dRNP-HTY3' with (900ng Amplicon) was ran at least two times.

I found evidence to support selective binding and detection of dRNP-MUT3' for SCD1 amplicon; however, there was no evidence to support selective binding and detection of dRNP-MUT3' for SCD1 amplicon. The average responses of the four amplicon samples (Healthy, SCD1, SCD2, and Scram) were different, with SCD1 amplicon sample with the highest average response at 10.94 and Scram amplicon sample with the lowest response at 4.75 (One-Way ANOVA: $F_{3, 35} = 11.38$, p = 2.33e-05, Fig. 6). A post-Tukey test was performed and further supports dRNP-HTY3' complex's higher affinity of binding with SCD1 sample. While the average I-Responses of SCD1 and SCD2 are similar, there is no statistical significance between average I-Responses

between SCD2 amplicon and Healthy amplicon (Post-Tukey: p-adj = 0.7444647). The results are shown in the Table 3 (* notes statistical significance).

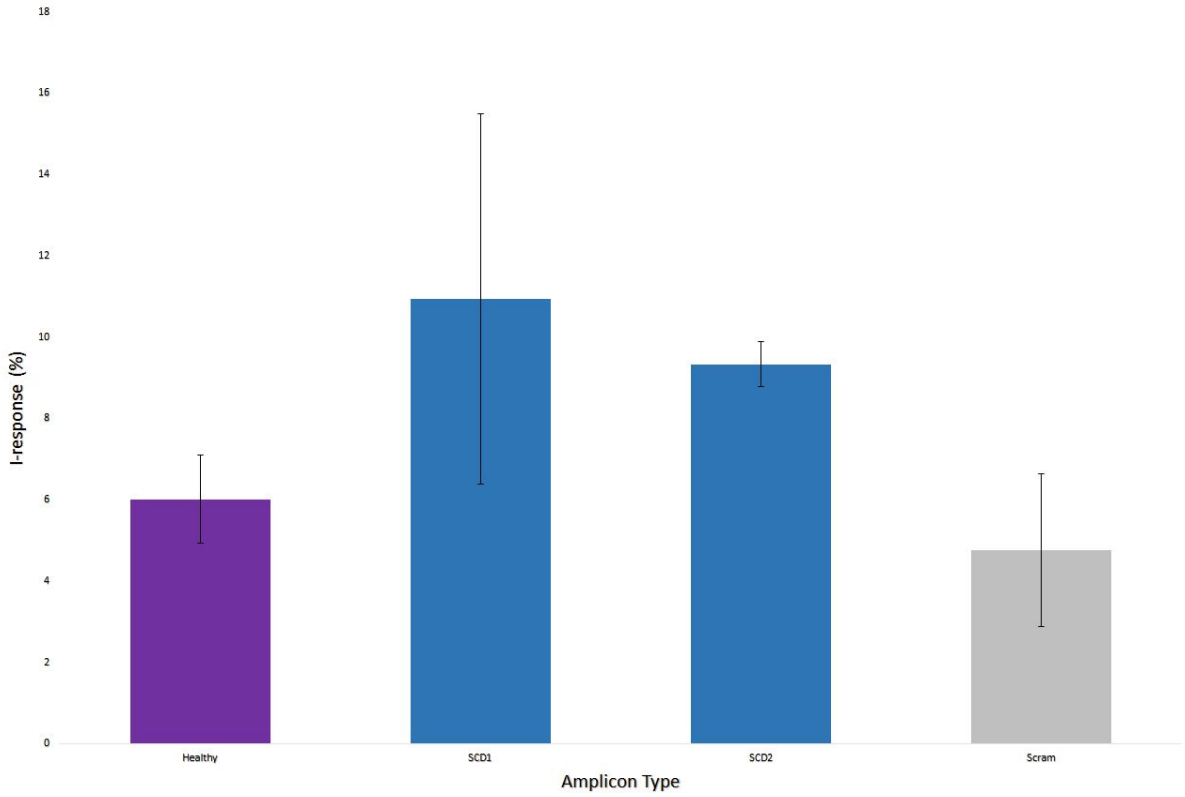

Figure 6. The relationship between dRNP-MUT3' (900ng amplicon type) and average I-Response (%). Bar heights and bars represent means ± standard deviation. Healthy (n=9), SCD1 (n=12), SCD2 (n=6), Scram (n=12) (n= number of working transistors).

Table 3. Post-Tukey analysis of dRNP-MUT3' sensor responses of amplicon samples

Amplicon Comparison	P-adjusted value
Healthy-SCD1 *	0.0018922
Healthy-SCD2	0.1336568
Healthy-Scram	0.7444647
SCD1-SCD2	0.6687290
SCD1-Scram *	0.0000300
SCD2-Scram *	0.0130985

Conclusion and Future Directions

The use of gFET biosensors has become increasingly popular for detecting large molecules in biomedical, clinical, and environmental applications (Afsahi et al., 2018; Forsyth et al., 2017; Justino et al., 2017). The CRISPR-Chip, a gFET biosensor with immobilized catalytically inactivated CRISPR-Cas9 complex, was able to specifically detect target DNA sequences with and without the sickle cell disease-associated single nucleotide polymorphism in both amplicon and genomic samples. The CRISPR-Cas9 complex capturing mechanism is easily modifiable through sgRNA selection since the sgRNA chosen is target-specific.

As shown in the Results section, with the dRNP-HTY3' complex, the CRISPR-Chip was able to specifically detect the target sequences of healthy patient, with and without pre-amplification. With the dRNP-MUT3' complex, the CRISPR-Chip was able to specifically detect one of the amplified target sequences from a patient with sickle cell disease. The differences in average current response between the SCD1 and SCD2 samples could be due to patient-to-patient variation. For further testing of this possible patient variation, future directions would consist of including a third DNA sample of another patient with sickle cell disease, as well as conducting additional trials to detect a possible pattern of difference between the patient samples. It is also important to note that sgRNA-MUT3' is based off of sgRNA-HTY3', which has been previously used in literature. sgRNA-MUT3' and sgRNA-MUT5', which were modified to contain the SCD-associated SNP, may have unexpected off-target effects that could affect its binding with the target and non-target DNA sequences. The large range in standard deviation of average current could be attributed to chip-to-chip variability, as well as variation in enzyme activity due to the length of the assay.

Nonetheless, the collected data shows promising indications for CRISPR-Chip's ability to specifically detect and differentiate between DNA samples from a healthy individual and DNA samples from individuals who have sickle cell disease as there are obvious and statistically supported differences in average current responses. Future directions include conducting more data with additional trials as mentioned before, and to run experiments of the dRNP-MUT3' complex with genomic samples and of the dRNP-MUT5' complex with both amplicon and genomic samples.

Researched have already demonstrated CRISPR-Chip's promising diagnostic potential for genetic diseases with samples containing insertions (BFP) as well as with samples containing clinically relevant deletions (DMD) (Hajian et al., 2019). As sickle cell disease can already be diagnosed with a simple blood test at birth, CRISPR-Chip's capacity for SCD-associated SNP detection has potential as a gene-editing monitoring tool for both efficiency and efficacy. Facile detection, analysis, and editing of sickle cell disease using CRISPR-based editing and monitoring would be beneficial for simple diagnostic and gene-editing therapeutic treatment of other single nucleotide polymorphisms as well, such as beta-thalassemia and cystic fibrosis.

Acknowledgements

My greatest thanks to my first thesis reader, Dr. Kiana Aran, for her helpful guidance, patience, and insightful feedback with my thesis throughout the year. I would like to also thank my second thesis reader, Dr. John Milton, for his frequent check-ins and enthusiasm for my thesis. Thank you to Sarah Balderston, a research assistant in the lab, for her mentoring and feedback during the experimental design and writing processes. I would also like to thank the Keck Science Department and Keck Graduate Institute for providing me with this valuable educational opportunity and its necessary resources. Lastly, thank you to my friends and family for their encouragement and support.

References

Afsahi, S., Lerner, M.B., Goldstein, J.M., Lee, J., Tang, X., Bagarozzi, D.A., Pan, D., Locascio, L., Walker, A., Barron, F., Goldsmith, B.R., 2018. Novel graphene-based biosensor for early detection of Zika virus infection. Biosens. Bioelectron. 100, 85–88. https://doi.org/10.1016/j.bios.2017.08.051

Anders, C., Niewoehner, O., Duerst, A., Jinek, M., 2014. Structural basis of PAM-dependent target DNA recognition by the Cas9 endonuclease. Nature 513, 569–573. https://doi.org/10.1038/nature13579

Aryal, N.K., Wasylishen, A.R., Lozano, G., 2018. CRISPR/Cas9 can mediate high-efficiency off-target mutations in mice in vivo. Cell Death Dis. 9, 1099. https://doi.org/10.1038/s41419-018-1146-0

Bialk, P., Sansbury, B., Rivera-Torres, N., Bloh, K., Man, D., Kmiec, E.B., 2016. Analyses of point mutation repair and allelic heterogeneity generated by CRISPR/Cas9 and single-stranded DNA oligonucleotides. Sci. Rep. 6, 32681. https://doi.org/10.1038/srep32681

Boyle, E.A., Andreasson, J.O.L., Chircus, L.M., Sternberg, S.H., Wu, M.J., Guegler, C.K., Doudna, J.A., Greenleaf, W.J., 2017. High-throughput biochemical profiling reveals sequence determinants of dCas9 off-target binding and unbinding. Proc. Natl. Acad. Sci. U. S. A. 114, 5461–5466. https://doi.org/10.1073/pnas.1700557114

Cao, L., Cui, X., Hu, J., Li, Z., Choi, J.R., Yang, Q., Lin, M., Ying Hui, L., Xu, F., 2017. Advances in digital polymerase chain reaction (dPCR) and its emerging biomedical applications. Biosens. Bioelectron. 90, 459–474. https://doi.org/10.1016/j.bios.2016.09.082

Demirci, S., Uchida, N., Tisdale, J.F., 2018. Gene therapy for sickle cell disease: An update. Cytotherapy 20, 899–910. https://doi.org/10.1016/j.jcyt.2018.04.003

DeWitt, M.A., Magis, W., Bray, N.L., Wang, T., Berman, J.R., Urbinati, F., Heo, S.-J., Mitros, T., Muñoz, D.P., Boffelli, D., Kohn, D.B., Walters, M.C., Carroll, D., Martin, D.I., Corn, J.E., 2016. Selection-free Genome Editing of the Sickle Mutation in Human Adult Hematopoietic Stem/Progenitor Cells. Sci. Transl. Med. 8, 360ra134. https://doi.org/10.1126/scitranslmed.aaf9336

Everaerts, F., Torrianni, M., Hendriks, M., Feijen, J., 2008. Biomechanical properties of carbodiimide crosslinked collagen: influence of the formation of ester crosslinks. J. Biomed. Mater. Res. A 85, 547–555. https://doi.org/10.1002/jbm.a.31524

Ficht, S., Mattes, A., Seitz, O., 2004. Single-Nucleotide-Specific PNA−Peptide Ligation

on Synthetic and PCR DNA Templates. J. Am. Chem. Soc. 126, 9970–9981. https://doi.org/10.1021/ja048845o

Forsyth, R., Devadoss, A., Guy, O.J., 2017. Graphene Field Effect Transistors for Biomedical Applications: Current Status and Future Prospects. Diagn. Basel Switz. 7. https://doi.org/10.3390/diagnostics7030045

Fu, Y., Foden, J.A., Khayter, C., Maeder, M.L., Reyon, D., Joung, J.K., Sander, J.D., 2013. High-frequency off-target mutagenesis induced by CRISPR-Cas nucleases in human cells. Nat. Biotechnol. 31, 822–826. https://doi.org/10.1038/nbt.2623

Galgano, L., Hutt, D., 2018. HSCT: How Does It Work?, in: Kenyon, M., Babic, A. (Eds.), The European Blood and Marrow Transplantation Textbook for Nurses: Under the Auspices of EBMT. Springer International Publishing, Cham, pp. 23–36. https://doi.org/10.1007/978-3-319-50026-3_2

Gerion, D., Chen, F., Kannan, B., Fu, A., Parak, W.J., Chen, D.J., Majumdar, A., Alivisatos, A.P., 2003. Room-Temperature Single-Nucleotide Polymorphism and Multiallele DNA Detection Using Fluorescent Nanocrystals and Microarrays. Anal. Chem. 75, 4766–4772. https://doi.org/10.1021/ac034482j

Gupta, R.M., Musunuru, K., 2014. Expanding the genetic editing tool kit: ZFNs, TALENs, and CRISPR-Cas9. J. Clin. Invest. 124, 4154–4161. https://doi.org/10.1172/JCI72992

Hajian, R., Balderston, S., Tran, T., deBoer, T., Etienne, J., Sandhu, M., Wauford, N.A., Chung, J.-Y., Nokes, J., Athaiya, M., Paredes, J., Peytavi, R., Goldsmith, B., Murthy, N., Conboy, I.M., Aran, K., 2019. Detection of unamplified target genes via CRISPR–Cas9 immobilized on a graphene field-effect transistor. Nat. Biomed. Eng. 1. https://doi.org/10.1038/s41551-019-0371-x

Hoban, M.D., Lumaquin, D., Kuo, C.Y., Romero, Z., Long, J., Ho, M., Young, C.S., Mojadidi, M., Fitz-Gibbon, S., Cooper, A.R., Lill, G.R., Urbinati, F., Campo-Fernandez, B., Bjurstrom, C.F., Pellegrini, M., Hollis, R.P., Kohn, D.B., 2016. CRISPR/Cas9-Mediated Correction of the Sickle Mutation in Human CD34+ cells. Mol. Ther. 24, 1561–1569. https://doi.org/10.1038/mt.2016.148

Hsu, P.D., Scott, D.A., Weinstein, J.A., Ran, F.A., Konermann, S., Agarwala, V., Li, Y., Fine, E.J., Wu, X., Shalem, O., Cradick, T.J., Marraffini, L.A., Bao, G., Zhang, F., 2013. DNA targeting specificity of RNA-guided Cas9 nucleases. Nat. Biotechnol. 31, 827–832. https://doi.org/10.1038/nbt.2647

Hudecova, I., 2015. Digital PCR analysis of circulating nucleic acids. Clin. Biochem., Circulating Nucleic Acids 48, 948–956. https://doi.org/10.1016/j.clinbiochem.2015.03.015

Iyer, V., Boroviak, K., Thomas, M., Doe, B., Riva, L., Ryder, E., Adams, D.J., 2018. No unexpected CRISPR-Cas9 off-target activity revealed by trio sequencing of

gene-edited mice. PLOS Genet. 14, e1007503. https://doi.org/10.1371/journal.pgen.1007503

Jiang, F., Doudna, J.A., 2017. CRISPR–Cas9 Structures and Mechanisms. Annu. Rev. Biophys. 46, 505–529. https://doi.org/10.1146/annurev-biophys-062215-010822

Justino, C.I.L., Duarte, A.C., Rocha-Santos, T.A.P., 2017. Recent Progress in Biosensors for Environmental Monitoring: A Review. Sensors 17. https://doi.org/10.3390/s17122918

Kassim, A.A., Sharma, D., 2017. Hematopoietic stem cell transplantation for sickle cell disease: The changing landscape. Hematol. Oncol. Stem Cell Ther., SI:Proceedings of WBMT 10, 259–266. https://doi.org/10.1016/j.hemonc.2017.05.008

Lu, N., Gao, A., Dai, P., Song, S., Fan, C., Wang, Y., Li, T., 2014. CMOS-Compatible Silicon Nanowire Field-Effect Transistors for Ultrasensitive and Label-Free MicroRNAs Sensing. Small 10, 2022–2028. https://doi.org/10.1002/smll.201302990

Lux, C.T., Pattabhi, S., Berger, M., Nourigat, C., Flowers, D.A., Negre, O., Humbert, O., Yang, J.G., Lee, C., Jacoby, K., Bernstein, I., Kiem, H.-P., Scharenberg, A., Rawlings, D.J., 2019. TALEN-Mediated Gene Editing of HBG in Human Hematopoietic Stem Cells Leads to Therapeutic Fetal Hemoglobin Induction. Mol. Ther. - Methods Clin. Dev. 12, 175–183. https://doi.org/10.1016/j.omtm.2018.12.008

Moran, K., Ling, H., Lessard, S., Viera, B., Hong, V., Holmes, M.C., Reik, A., Dang, D., Gray, D., Levasseur, D., Rimmele, P., 2018. Ex Vivo Gene-Edited Cell Therapy for Sickle Cell Disease: Disruption of the BCL11A Erythroid Enhancer with Zinc Finger Nucleases Increases Fetal Hemoglobin in Plerixafor Mobilized Human CD34+ Cells. Blood 132, 2190. https://doi.org/10.1182/blood-2018-99-116998

Nakajima, K., Kazuno, A., Kelsoe, J., Nakanishi, M., Takumi, T., Kato, T., 2016. Exome sequencing in the knockin mice generated using the CRISPR/Cas system. Sci. Rep. 6, 34703. https://doi.org/10.1038/srep34703

Park, S.H., Lee, C.M., Deshmukh, H., Bao, G., 2016. Therapeutic Crispr/Cas9 Genome Editing for Treating Sickle Cell Disease. Blood 128, 4703.

Pattanayak, V., Lin, S., Guilinger, J.P., Ma, E., Doudna, J.A., Liu, D.R., 2013. High-throughput profiling of off-target DNA cleavage reveals RNA-programmed Cas9 nuclease specificity. Nat. Biotechnol. 31, 839–843. https://doi.org/10.1038/nbt.2673

Peña-Bahamonde, J., Nguyen, H.N., Fanourakis, S.K., Rodrigues, D.F., 2018. Recent advances in graphene-based biosensor technology with applications in life sciences. J. Nanobiotechnology 16, 75.

https://doi.org/10.1186/s12951-018-0400-z

Ping, J., Vishnubhotla, R., Vrudhula, A., Johnson, A.T.C., 2016. Scalable Production of High-Sensitivity, Label-Free DNA Biosensors Based on Back-Gated Graphene Field Effect Transistors. ACS Nano 10, 8700–8704. https://doi.org/10.1021/acsnano.6b04110

Pumera, M., 2011. Graphene in biosensing. Mater. Today 14, 308–315. https://doi.org/10.1016/S1369-7021(11)70160-2

Ribeil, J.-A., Hacein-Bey-Abina, S., Payen, E., Magnani, A., Semeraro, M., Magrin, E., Caccavelli, L., Neven, B., Bourget, P., El Nemer, W., Bartolucci, P., Weber, L., Puy, H., Meritet, J.-F., Grevent, D., Beuzard, Y., Chrétien, S., Lefebvre, T., Ross, R.W., Negre, O., Veres, G., Sandler, L., Soni, S., de Montalembert, M., Blanche, S., Leboulch, P., Cavazzana, M., 2017. Gene Therapy in a Patient with Sickle Cell Disease. N. Engl. J. Med. 376, 848–855. https://doi.org/10.1056/NEJMoa1609677

Sebastiano, V., Maeder, M.L., Angstman, J.F., Haddad, B., Khayter, C., Yeo, D.T., Goodwin, M.J., Hawkins, J.S., Ramirez, C.L., Batista, L.F.Z., Artandi, S.E., Wernig, M., Joung, J.K., 2011. In situ genetic correction of the sickle cell anemia mutation in human induced pluripotent stem cells using engineered zinc finger nucleases. Stem Cells Dayt. Ohio 29, 1717–1726. https://doi.org/10.1002/stem.718

Sun, N., Zhao, H., 2014. Seamless correction of the sickle cell disease mutation of the HBB gene in human induced pluripotent stem cells using TALENs. Biotechnol. Bioeng. 111, 1048–1053. https://doi.org/10.1002/bit.25018

Tasan, I., Jain, S., Zhao, H., 2016. Use of Genome Editing Tools to Treat Sickle Cell Disease. Hum. Genet. 135, 1011–1028. https://doi.org/10.1007/s00439-016-1688-0

Tsai, S.Q., Nguyen, N.T., Malagon-Lopez, J., Topkar, V.V., Aryee, M.J., Joung, J.K., 2017. CIRCLE-seq: a highly sensitive *in vitro* screen for genome-wide CRISPR–Cas9 nuclease off-targets. Nat. Methods 14, 607–614. https://doi.org/10.1038/nmeth.4278

Wang, C., Yan, Q., Liu, H.-B., Zhou, X.-H., Xiao, S.-J., 2011. Different EDC/NHS Activation Mechanisms between PAA and PMAA Brushes and the Following Amidation Reactions. Langmuir 27, 12058–12068. https://doi.org/10.1021/la202267p

Wang, H., Yang, H., Shivalila, C.S., Dawlaty, M.M., Cheng, A.W., Zhang, F., Jaenisch, R., 2013. One-Step Generation of Mice Carrying Mutations in Multiple Genes by CRISPR/Cas-Mediated Genome Engineering. Cell 153, 910–918. https://doi.org/10.1016/j.cell.2013.04.025

Xiao, Y., Plakos, K.J.I., Lou, X., White, R.J., Qian, J., Plaxco, K.W., Soh, H.T., 2009.

Fluorescence Detection of Single-Nucleotide Polymorphisms with a Single, Self-Complementary, Triple-Stem DNA Probe. Angew. Chem. Int. Ed. 48, 4354–4358. https://doi.org/10.1002/anie.200900369